

Properties of human glycine receptors containing the hyperekplexia mutation $\alpha 1(K276E)$, expressed in *Xenopus* oocytes

T. M. Lewis, L. G. Sivilotti, D. Colquhoun, R. M. Gardiner*, R. Schoepfer † and M. Rees*

*Department of Pharmacology, † Wellcome Laboratory for Molecular Pharmacology and *Department of Paediatrics, University College London, Gower Street, London WC1E 6BT, UK*

(Received 30 May 1997; accepted after revision 10 October 1997)

1. Inherited defects in human glycine receptors give rise to hyperekplexia (startle disease). We expressed human glycine receptors in *Xenopus* oocytes, in order to examine the pharmacological and single-channel properties of receptors that contain a mutation, $\alpha 1(K276E)$, associated with an atypical form of hyperekplexia.
2. Equilibrium concentration–response curves showed that recombinant human $\alpha 1(K276E)\beta$ receptors had a 29-fold lower glycine sensitivity than wild-type $\alpha 1\beta$ receptors, and a greatly reduced Hill coefficient. The maximum response to glycine also appeared much reduced, whereas the equilibrium constant for the glycine receptor antagonist strychnine was unchanged.
3. Both wild-type and mutant channels opened to multiple conductance levels with similar main conductance levels (33 pS) and weighted mean conductances (41.5 versus 49.8 pS, respectively).
4. Channel openings were shorter for the $\alpha 1(K276E)\beta$ mutant than for the wild-type $\alpha 1\beta$, with mean overall apparent open times of 0.82 and 6.85 ms, respectively.
5. The main effect of the $\alpha 1(K276E)$ mutation is to impair the opening of the channel rather than the binding of glycine. This is shown by the results of fitting glycine dose–response curves with particular postulated mechanisms, the shorter open times of mutant channels, the properties of single-channel bursts, and the lack of an effect of the mutation on the strychnine-binding site.

Hyperekplexia, or startle disease, is a rare neurological condition, which is usually inherited in an autosomal dominant manner and is associated with mutations in the gene (*GLRA1*) for the $\alpha 1$ subunit of the glycine receptor on human chromosome 5 (exons 6 and 7; Shiang, Ryan, Zhu, Hahn, O'Connell & Wasmuth, 1993; Rees, Andrew, Jawad & Owen, 1994; Schorderet, Pescia, Bernasconi & Regli, 1994; Rajendra & Schofield, 1995; Shiang *et al.* 1995; Brune *et al.* 1996). The disease is characterized by severe neonatal hypertonia (which can precipitate life-threatening apnoea) and an exaggerated startle response to unexpected auditory or tactile stimuli (Kurczynski, 1983; Vigevano, Di Capua & Dalla Bernardina, 1989; Nigro & Lim, 1992). If patients survive this period, the hypertonia diminishes, although the startle response persists into adulthood. Treatment with the benzodiazepine clonazepam is effective at reducing both the neonatal hypertonia and the magnitude of the startle response (Ryan, Sherman, Terry, Sparkes, Torres & Mackey, 1992).

An atypical form of familial hyperekplexia, associated with spasticity of the lower limbs, is also linked to chromosome 5 (Baxter *et al.* 1996): affected individuals in this pedigree are heterozygous for a single A to G point mutation (in exon 6), which is predicted to result in the substitution of the normal lysine residue with glutamic acid in position 276 of the glycine $\alpha 1$ subunit (K276E; Elmslie *et al.* 1996).

Heterologous expression studies of recombinant glycine receptors have shown that introducing any of the startle disease mutations (I244N, R271L/Q, Y279C and K276E) in the $\alpha 1$ subunit has profound effects on receptor function, producing, for example, substantial increases in the EC_{50} for glycine (Langosch, Laube, Rundström, Schmieden, Bormann & Betz, 1994; Rajendra, Lynch, Pierce, French, Barry & Schofield, 1994; Lynch, Rajendra, Pierce, Handford, Barry & Schofield, 1997). In the case of the extensively studied R271 mutants, there is also a reduction in the average single-channel conductance (Langosch *et al.* 1994; Rajendra *et al.* 1994). The occurrence of four of the hyperekplexia

mutations (R271L/Q, Y279C and K276E) within the short extracellular loop between the second and third of the predicted membrane-spanning regions (M2 and M3) of the $\alpha 1$ subunit protein, has raised questions as to the function of this region.

The aim of the present work was to extend the functional study of recombinant human $\alpha 1$ (K276E) mutants to heteromeric ($\alpha 1\beta$) receptors, which are likely to constitute the majority of adult native glycine receptors (Langosch, Thomas & Betz, 1988), and to investigate the reasons for their impaired function at the single-channel level. Our results show that the startle disease mutation $\alpha 1$ (K276E) increased the EC_{50} and reduced the maximum response of recombinant heteromeric $\alpha 1\beta$ glycine receptors without altering their sensitivity to strychnine; single-channel conductance was unchanged, but the mean duration of channel openings was markedly reduced.

Identification of the step in the activation of a receptor which is affected by a mutation cannot be done rigorously without a quantitative description of receptor behaviour in terms of rate constants for each reaction step, i.e. it is inherently model dependent (e.g. Colquhoun & Farrant, 1993). Because there is no generally accepted mechanism for the glycine receptor, we have tested several different plausible mechanisms. Each of them fits the data quite well. Perhaps surprisingly, all of them lead to the same qualitative conclusion, namely that the binding of glycine to the shut state of the channel was not greatly affected by the mutation, but that the ability of the occupied receptor to open was greatly impaired. This qualitative conclusion, therefore, seems to be quite robust. More quantitative conclusions will require much more work on the receptor mechanism.

METHODS

Site-directed mutagenesis and expression of human glycine receptors

The cDNAs coding for the human $\alpha 1$ subunit (a gift from H. Betz, Abteilung Neurochemie, Max-Planck-Institut für Hirnforschung, Frankfurt, Germany; Grenningloh *et al.* 1990) and the β subunit (a gift from P. Schofield, Garvan Institute of Medical Research, Sydney, Australia; Handford *et al.* 1996) of the human glycine receptor were each subcloned into a pSP64T-derived expression vector (Krieg & Melton, 1984). In these constructs all of the 5' and most of the 3' untranslated segments from the glycine receptor subunits were replaced with vector-encoded *Xenopus* globin 5' untranslated segments, followed by a Kozak consensus sequence ACCATG (initiating ATG – for Met – in bold), and by *Xenopus* globin 3' untranslated regions (vector encoded), respectively. In order to facilitate cloning, the triplet following the initiating ATG was changed to ACC, coding for the amino acid Thr, in the case of the $\alpha 1$ subunit, and to GCG (Gly) in the case of the β subunit. An A to G base substitution corresponding to K276E was introduced at nucleotide position 1206 of the $\alpha 1$ subunit construct, using the polymerase chain reaction, and verified by DNA sequencing of the relevant segments. Complementary RNA (cRNA) was then transcribed using T7 RNA polymerase and rNTPs (RiboMax kit,

Promega) supplemented with the 5' cap analogue, m7G(5')ppp(5')G (Pharmacia Biotech, Uppsala, Sweden). The integrity and approximate concentration of the cRNA was determined by electrophoresis on denaturing agarose (1%) gels and staining with ethidium bromide. Mixtures of wild-type $\alpha 1$ and $\alpha 1$ (K276E) with the β subunit were initially prepared at ratios of 4:1, 1:1, 1:4 and 1:10 (α : β) to check for the incorporation of the β subunit, after which the 1:4 ratio was routinely used for the experiments.

Mature, female *Xenopus laevis* frogs were anaesthetized by immersion in neutralized ethyl *m*-aminobenzoate solution (tricaine methanesulphonate salt; 0.2% solution w/v; Sigma), and killed by decapitation and destruction of the brain and spinal cord before removal of ovarian lobes. Clumps of five to eight stage V–VI oocytes were dissected in a sterile modified Barth's solution of composition (mM): NaCl, 88; KCl, 1; MgCl₂, 0.82; Ca(NO₃)₂, 0.33; CaCl₂, 0.44; NaHCO₃, 2.4; Tris-HCl, 15; with 50 U ml⁻¹ penicillin and 50 μ g ml⁻¹ streptomycin; pH 7.4. The dissected oocytes were treated with collagenase (Type IA, Sigma; 75 min at 19 °C, 245 U ml⁻¹ in Barth's solution, ten to twelve oocytes per millilitre), rinsed, and defolliculated (usually 12–18 h later) before cRNA injection (23 nl per oocyte). The oocytes were incubated for 2 days at 19 °C, screened for GlyR expression, then stored at 4 °C for up to 14 days after injection. All experiments were conducted at a controlled room temperature of 18–20 °C.

Whole-cell responses

Whole-cell currents were recorded from oocytes using standard two-microelectrode voltage-clamp techniques (Geneclamp 500 amplifier, Axon Instruments) at a holding potential of –80 mV. The bath solution was clamped actively to ground potential, with 3 M KCl agar (3%) bridges connected via Ag–AgCl pellets for both the sensor and bath electrodes. Recording microelectrodes were filled with 2 M potassium acetate, acidified with 100 mM HCl (to pH 6.2), and had resistances of 3–5 M Ω . Whole-cell currents were played out onto a chart recorder during the experiment and recorded onto digital audio tape (Biologic, DTR-1204). The oocytes were mounted in a small volume bath (200 μ l), within a 'funnel' of four insect pins on a Sylgard 184 (Dow Corning) base. The inflow for bath perfusion was divided at a 'Y' branch and directed onto the oocyte from directly opposite sides through 1.5 mm diameter glass capillaries. Solutions were superfused at a rate of about 10 ml min⁻¹ for concentration–response experiments or 2 ml min⁻¹ for low-concentration equilibrium responses in the presence of strychnine. The normal bathing solution was of composition (mM): NaCl, 150; KCl, 2.8; CaCl₂, 2; MgCl₂, 1; Hepes, 10; pH 7.4 adjusted with NaOH. Changes in solution were effected by manually switching a Hamilton 3-way tap upstream of the 'Y' junction. Glycine was purchased from Fluka Chemie AG (BioChemika grade) and picrotoxin was purchased from RBI.

As in all such studies, the determination of the equilibrium response was made somewhat dubious by desensitization, and the peak response (measured from the chart record) to glycine was used as an approximation. A minimum of 4 min was allowed between successive agonist applications. Before pooling, responses were normalized to a near-maximum response elicited by a concentration of glycine that was common to all sets. The responses, y , to glycine concentration $[A]$, were fitted empirically with the Hill equation

$$y = y_{\max} \frac{[A]^{n_H}}{[A]^{n_H} + EC_{50}^{n_H}}, \quad (1)$$

where y_{\max} is the maximum response, EC_{50} is the agonist concentration for 50% maximum response and n_H is the Hill coefficient.

Strychnine antagonism was examined by the Schild method (Schild, 1949; Arunlakshana & Schild, 1959). On individual oocytes, two- or three-point concentration–response curves to glycine were determined first; similar responses were then obtained in the presence of 50, 100, 300 and 1000 nM strychnine hydrochloride (Sigma) by appropriately increasing the concentration of glycine applied. Small responses were used in order to minimize desensitization. The oocytes were equilibrated at each strychnine concentration for 4 min before the co-application of glycine. The low-concentration–response curves were fitted simultaneously with power functions that were constrained to be parallel to allow dose ratios, r , to be estimated for each concentration of strychnine. Separate unconstrained fits to each individual curve were done to judge the adequacy of parallelism. The mean dose ratios for each concentration of strychnine were fitted by the Schild equation

$$r - 1 = [B]/K_B, \quad (2)$$

which is also linear in its logarithmic form:

$$\log(r - 1) = \log[B] - \log K_B,$$

where $[B]$ is the concentration of antagonist and K_B is its dissociation equilibrium constant. The Schild plot ($\log(r - 1)$ versus $\log[B]$) was fitted, not in the logarithmic form but by fitting the $(r - 1)$ and $[B]$ values with

$$(r - 1) = a[B]^n,$$

where a is a constant, n is the slope of the Schild plot, which is predicted by the Schild equation to be unity for a competitive antagonist at equilibrium. If n was sufficiently close to one, then the results were taken to be consistent with the Schild equation, so the data were re-fitted with the slope constrained to one (i.e. re-fitted with the Schild equation) for estimation of K_B .

Single-channel recordings

Before patch-clamp recording from oocytes, the vitelline membrane was removed by fine dissection after exposing the oocyte to hypertonic solution of composition (mM): sodium methylsulphate, 200; KCl, 20; Hepes, 10; MgCl₂, 1; adjusted to pH 7.4 with KOH. Recordings were made in the same normal bath solution as above, using an Axopatch-1B amplifier (Axon Instruments) with a DB-1 electrode holder (G23 Instruments, Department of Pharmacology, University College London), and agonist was applied in the bath solution. Outside-out patches were used to allow unequivocal identification of glycine-activated channels. Patch pipettes were fabricated on a vertical puller (List Medical, L/M-3P-A) from thick-walled borosilicate glass (GC150F, Clark Electromedical Instruments), coated with Sylgard 184 (Dow Corning) and fire-polished before use to a final resistance of 8–10 M Ω . The pipettes were filled with an internal solution of composition (mM): CsCl, 120; TEA-Cl, 20; CaCl₂, 1; MgCl₂, 2; Hepes, 10; EGTA, 11; adjusted to pH 7.2 with CsOH. Single-channel currents were low-pass filtered at 20 kHz (4-pole Bessel, –3 dB) and stored on FM tape (Store 4, Racal) at a tape speed of 15 in s^{–1} (bandwidth DC to 5 kHz, Tchebychev filter) to be analysed off-line.

Analysis of single-channel recordings

Records were digitized at 15–30 kHz (CED-1401plus interface, Cambridge Electronic Design, Cambridge, UK) after filtering at 1.5–3 kHz (8-pole Bessel, –3 dB). Single-channel events were analysed by the method of time course fitting with the program SCAN (Colquhoun & Sigworth, 1995). Sections of recordings with simultaneous openings of more than one channel were excised from the analysis, and patches in which these excised sections contributed 10% or more of the openings were discarded, in order

to prevent length-biased sampling from affecting the dwell time distributions. A fixed time resolution was imposed on the open and shut times found in SCAN before analysis of distributions, using a false-event rate criterion of less than 10^{–8} s^{–1}, taking into account the pre-filtering, amplitude of the full opening and baseline r.m.s. noise (Colquhoun & Hawkes, 1994).

For the purposes of dwell time distributions, we define an open period as the period between two adjacent shut periods (each longer than the resolution), i.e. as a period during which the channel appeared to be continuously open, regardless of possible transitions between different open levels. Within each open period, changes in the open amplitude were considered as transitions to a different level only if the difference in amplitude was greater than 0.6 pA. In this case, each of the openings to a different level – within the same open period – contributed one value to the distribution of amplitudes, provided the events were longer than three times the filter rise time. If changes in amplitude of less than 0.6 pA had been fitted as transitions in the first stage of analysis, the openings on each side of such transitions were concatenated into a single open period, to which was assigned an amplitude calculated as the mean amplitude (weighted by their duration) of the individual openings. Amplitude histograms were fitted with Gaussian distributions by the method of maximum likelihood. Distributions of logarithm of the open period and shut time durations were displayed using the square root of event frequency (Sigworth & Sine, 1987), and fitted with a mixture of exponential densities (areas a_i , time constants τ_i) by the method of maximum likelihood (EKDIST program; Colquhoun & Sigworth, 1995). The overall mean duration, $\sum a_i \tau_i$, was calculated from such fits.

Bursts of openings were examined on those records that were deemed to be suitable, on the basis of the separation of components in the shut time distribution. A critical shut time, t_{crit} was determined, such that the shortest component in the shut time distributions fell within bursts, using in the calculation the criterion of equal proportions of misclassified intervals (Colquhoun & Sakmann, 1985). The bursts of openings so defined were used to construct distributions of the burst durations and of the total open time per burst.

RESULTS

Equilibrium concentration–response curves

Both the wild-type $\alpha 1$ and the $\alpha 1(K276E)$ subunits were expressed homomericly, and as heteromers with the β subunit. Examples of the whole-cell currents in response to the application of glycine are shown in Fig. 1. It is immediately apparent that the $\alpha 1(K276E)$ homomeric and $\alpha 1(K276E)\beta$ receptors produce much smaller whole-cell currents than the wild-type $\alpha 1$ homomeric and $\alpha 1\beta$ receptors, for the same amount of injected cRNA. The time courses of the responses were also different for wild-type and mutant receptors. The wild-type receptors show a greater degree of ‘desensitization’ of the current following the peak response, in the continued presence of agonist, compared with the mutant receptors. This is, as usual, bound to result in some distortion of the concentration–response curves. Application of glycine concentrations up to 500 mM to uninjected oocytes or to oocytes expressing the β subunit alone did not result in any glycine-activated currents, nor any other (e.g. osmotically activated) currents.

Table 1. Parameters estimated from the fit of the Hill equation

Receptor	I_{\max} (μA)	EC_{50} (μM)	n_{H}	Oocytes (no.)
$\alpha 1$	6.15 ± 1.89	224.9 ± 8.43	3.20 ± 0.17	4
$\alpha 1\beta$	6.60 ± 1.72	187.1 ± 13.54	2.63 ± 0.14	5
$\alpha 1(\text{K}276\text{E})$	0.159 ± 0.011	3193 ± 272	1.16 ± 0.08	4
$\alpha 1(\text{K}276\text{E})\beta$	0.675 ± 0.318	5356 ± 596	1.32 ± 0.07	4

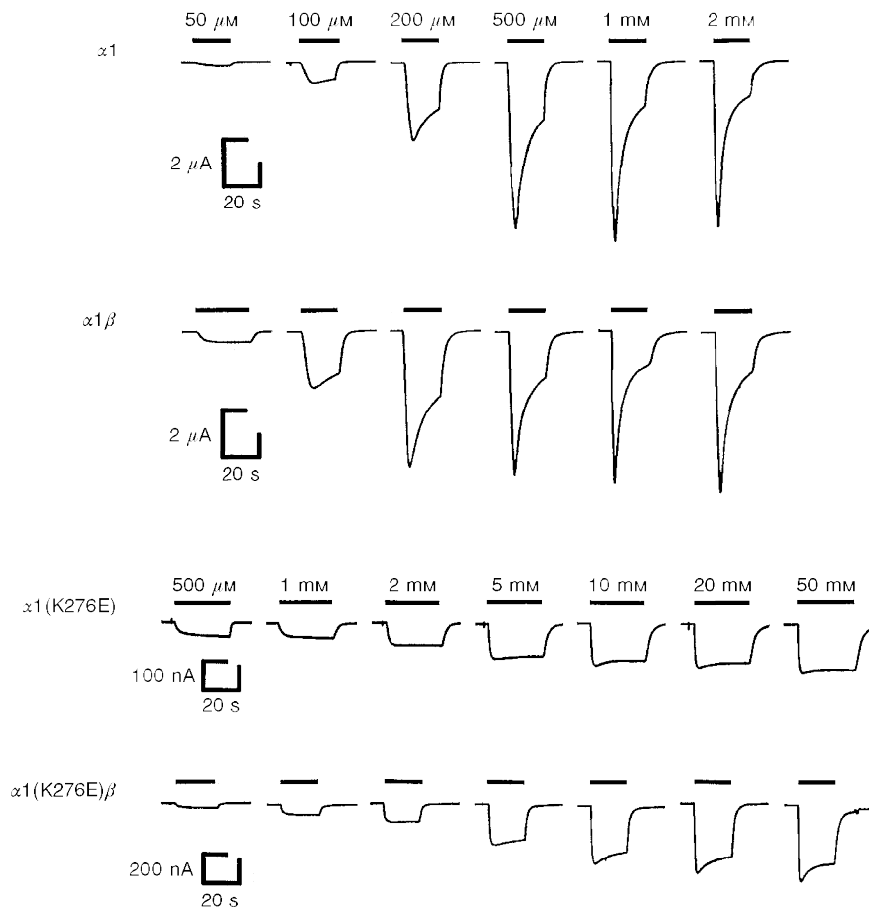
Values are expressed as means \pm s.d. of mean. For both the heteromeric subunit combinations, cRNAs for the α and β subunits were injected in the ratio 1:4.

The normalized concentration–response curves for both wild-type and mutant receptors, obtained from the pooled data from at least four separate oocytes in each case, are shown in Fig. 2, with their fitted Hill equations. The fitted parameters are summarized in Table 1. The mean maximum current for $\alpha 1(\text{K}276\text{E})\beta$ was 10-fold smaller than that for $\alpha 1\beta$ and the concentration–response curve for the mutant was shifted to the right, with an EC_{50} which was 29-fold

greater than that of the wild-type $\alpha 1\beta$. For the homomeric receptors, the EC_{50} was increased 14-fold by the mutation. For both homomeric and heteromeric receptors, the Hill coefficients of the dose–response curves obtained from the mutant receptors were considerably lower than for the wild-type receptors.

Affinity for strychnine

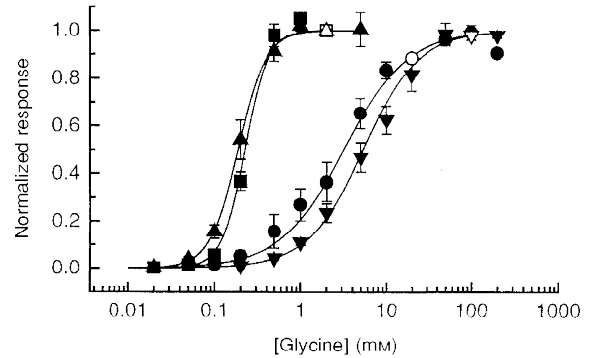
The competitive antagonist, strychnine, is known to bind at a site which overlaps with the glycine-binding site. Glycine and strychnine are reported to interact with different, yet neighbouring residues; for example, strychnine interacts with Lys-200 and Tyr-202, whilst glycine interacts with Thr-204 (Ruiz-Gomez, Morato, Garcia-Calco, Valdivieso & Mayor, 1990; Vandenberg, French, Barry, Shine & Schofield, 1992). Therefore the equilibrium constant (K_{B}) for strychnine binding was determined by the method of Schild as an indirect test for structural changes near the glycine-binding site caused by the K276E mutation. Little change was observed in the K_{B} for strychnine between $\alpha 1\beta$ ($K_{\text{B}} = 28 \text{ nM}$) and $\alpha 1(\text{K}276\text{E})\beta$ ($K_{\text{B}} = 23 \text{ nM}$), as shown in Fig. 3.

**Figure 1. Examples of glycine-activated currents**

Homomeric $\alpha 1$ or heteromeric $\alpha 1\beta$ (ratio 1:4) glycine receptors produced large inward currents in response to the application of glycine, reaching a maximum near 1 mM glycine (top two traces). Mutant $\alpha 1(\text{K}276\text{E})$ and $\alpha 1(\text{K}276\text{E})\beta$ (ratio 1:4) receptors required higher concentrations of glycine to activate inward currents, reaching a 10- to 40-fold smaller maximum near 50 mM glycine.

Figure 2. Averaged concentration–response curves

Shown here are the averaged data for wild-type $\alpha 1$ (■) and $\alpha 1\beta$ (▲), and for mutant $\alpha 1(K276E)$ (●) and $\alpha 1(K276E)\beta$ (▼). The continuous line is the fit of the Hill equation. In each case the corresponding open symbols represent the response used to normalize the data and therefore not included when fitting the data.



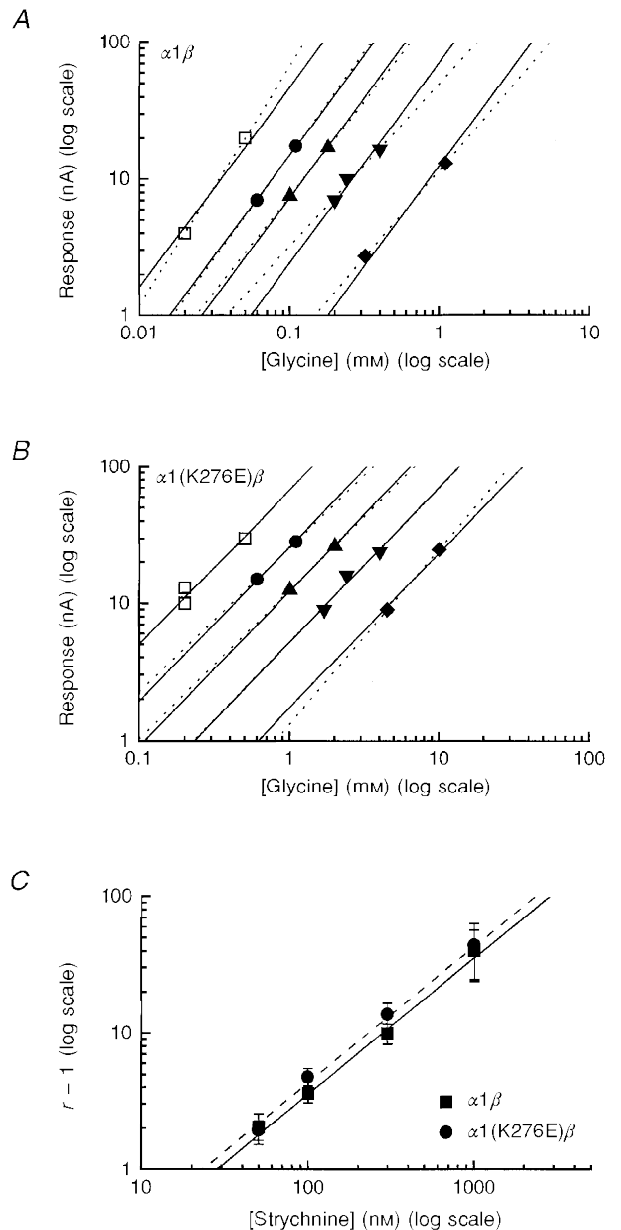
Incorporation of the β subunit

Initially the cRNAs for the heteromeric glycine receptor were mixed in ratios 4:1, 1:1, 1:4 and 1:10 (ratio α : β), and, following injection into oocytes, the expressed receptor population was screened for the incorporation of the β subunit by testing for sensitivity to picrotoxin. It has

previously been shown that heteromeric glycine receptors with the β subunit are less sensitive to picrotoxin than homomeric $\alpha 1$ receptors (Pribilla, Takagi, Langosch, Bormann & Betz, 1994). While the wild-type receptors demonstrated significant incorporation of the β subunit at a ratio of 1:1, an increase in the proportion of injected β cRNA

Figure 3. Strychnine antagonism of glycine responses

A and *B* show examples of responses to glycine in the absence of strychnine (□), and in the presence of 50 nM (●), 100 nM (▲), 300 nM (▼) and 1000 nM (◆) strychnine; obtained from oocytes expressing either $\alpha 1\beta$ (*A*) or $\alpha 1(K276E)\beta$ (*B*) glycine receptors. Continuous lines show the simultaneous fits of power functions constrained to be parallel, and dotted lines show separate unconstrained fits. From results such as these, dose ratios were estimated for each concentration of strychnine. *C*, Schild plot obtained from the dose ratio data for $\alpha 1\beta$ ($K_B = 28.1 \pm 2.7$ nM; slope, 0.949 ± 0.14 ; $n = 3$) and $\alpha 1(K276E)\beta$ ($K_B = 23.1 \pm 2.2$ nM; slope, 1.06 ± 0.10 ; $n = 3$) glycine receptors.



to 1:4 and to 1:10 had no further effect on picrotoxin sensitivity (data not shown). However, no difference in the picrotoxin sensitivity was observed between homomeric $\alpha 1(K276E)$ and $\alpha 1(K276E)\beta$: both had a sensitivity similar to that of the heteromeric wild-type receptor. It was also observed (data not shown) that low concentrations of picrotoxin could produce a potentiation of the glycine response for both homomeric and heteromeric mutant receptors, in a similar manner to that reported for the hyperkplexia mutation $\alpha 1(R271Q)$ (expressed homomericly; Lynch, Rajendra, Barry & Schofield, 1995). Therefore picrotoxin has limited usefulness as a tool for demonstrating the incorporation of the β subunit in mutant receptors. The results with the wild-type $\alpha 1\beta$ receptor, however, provide an indication of the ratio at which most receptors are heteromeric. This was also in agreement with a previous report on cRNA ratios in oocytes (Kuhse, Laube, Magalei & Betz, 1993). Thus the ratio of 1:4 was used for both wild-type and mutant glycine receptors and the single-channel amplitudes were sampled, looking for a redistribution to lower conductance levels with heteromeric receptors compared with homomeric, as has been previously shown (Bormann, Rundström, Betz & Langosch, 1993).

Single-channel responses

From the initial inspection of single-channel records like those shown in Fig. 4, it was clear that there was no radical decrease in the conductance of $\alpha 1(K276E)\beta$ receptors, of the sort seen with the R271Q hyperkplexia mutation (Langosch *et al.* 1994; Rajendra, Lynch, Pierce, French, Barry & Schofield, 1995). However, the $\alpha 1(K276E)\beta$ single-channel events appeared to be much shorter in duration.

The distributions of single-channel amplitudes recorded from wild-type $\alpha 1\beta$ and $\alpha 1(K276E)\beta$ outside-out patches held at -100 mV showed multiple conductance states, giving rise to current amplitudes between 2 and 9 pA for both combinations (Fig. 5A and C), though not all conductance states were present in every patch (which suggests that the recombinant receptors were not always homogenous). The most frequent amplitude component was 3.3 ± 0.1 pA (3.32 ± 0.16 pA for $\alpha 1\beta$ and 3.25 ± 0.07 pA for $\alpha 1(K276E)\beta$, $n = 6$ and 4, respectively; Fig. 5B). In a few patches, particularly of $\alpha 1(K276E)\beta$, the predominant amplitude was higher (7–8.5 pA). This higher conductance level, which also occurred at low frequency in other $\alpha 1\beta$ and $\alpha 1(K276E)\beta$ patches, is similar to that of homomeric

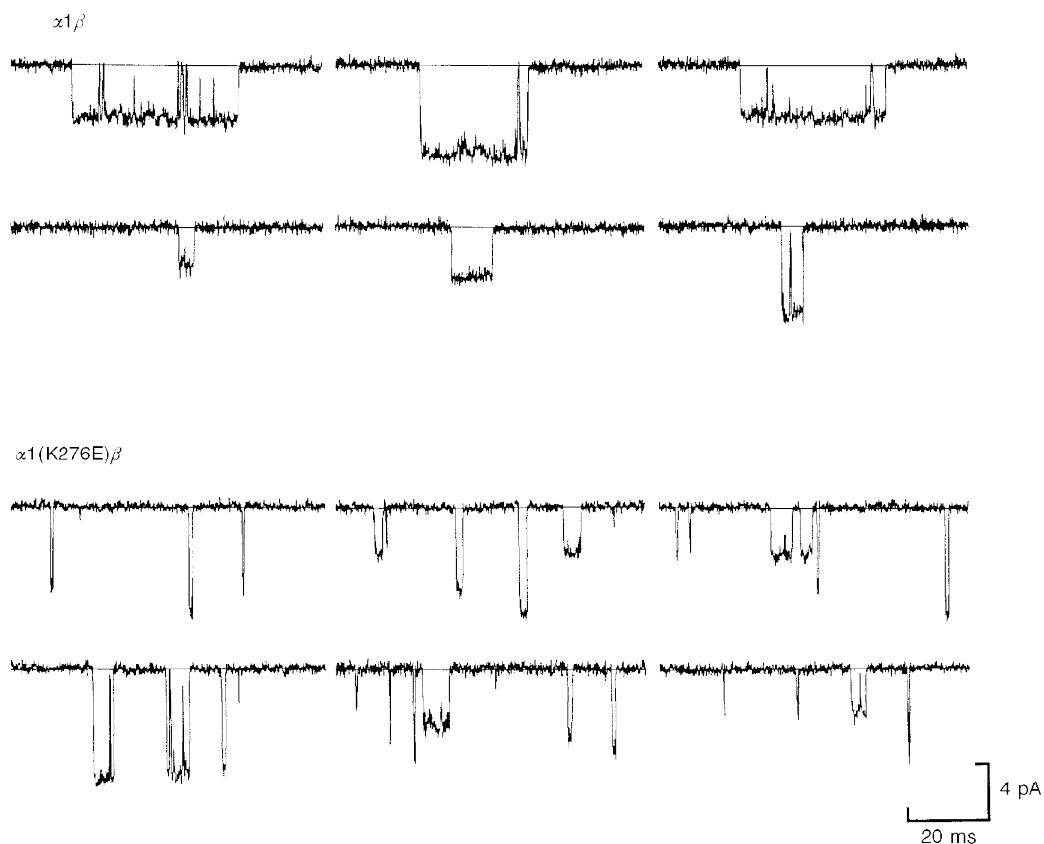


Figure 4. Examples of single-channel openings of $\alpha 1\beta$ and $\alpha 1(K276E)\beta$ glycine receptors

Records are currents obtained from outside-out patches (held at -100 mV; 3 kHz filter) in response to the application of glycine ($10 \mu\text{M}$ and $100 \mu\text{M}$ for wild-type and $\alpha 1(K276E)\beta$ receptors, respectively). Note that mutant receptors open to a range of conductance levels similar to that of wild-type receptors, but that the openings are shorter.

receptors (Bormann *et al.* 1993; our data, not shown), suggesting some degree of contamination by homomeric receptors.

An average chord conductance was calculated, each conductance being weighted with its relative area from the fit of a mixture of Gaussian densities, to give an indication of the transfer of charge through open $\alpha 1\beta$ and $\alpha 1(K276E)\beta$ glycine receptors. The reversal potential was assumed to be 0 mV (E_{Cl} was -2.1 mV with our internal and external solutions). For the wild-type $\alpha 1\beta$, the average chord conductance so calculated was 41.5 ± 6.5 pS and for $\alpha 1(K276E)\beta$ it was 49.8 ± 5.3 pS.

Distributions of open periods

Open period distributions of $\alpha 1\beta$ single-channel events could all be fitted with a mixture of three exponential densities (Fig. 6A). Most of the $\alpha 1(K276E)\beta$ open period distributions were also fitted with a mixture of three exponential densities (Fig. 6B), although three recordings lacked a well-defined fast component that was close to the imposed resolution of $60 \mu s$. A summary of the fitted parameters for the open period distributions is presented in Table 2. For each of the exponential densities fitted to the $\alpha 1\beta$ open periods, the mean time constants (τ_1 , τ_2 and τ_3) are each approximately five times larger than those fitted to

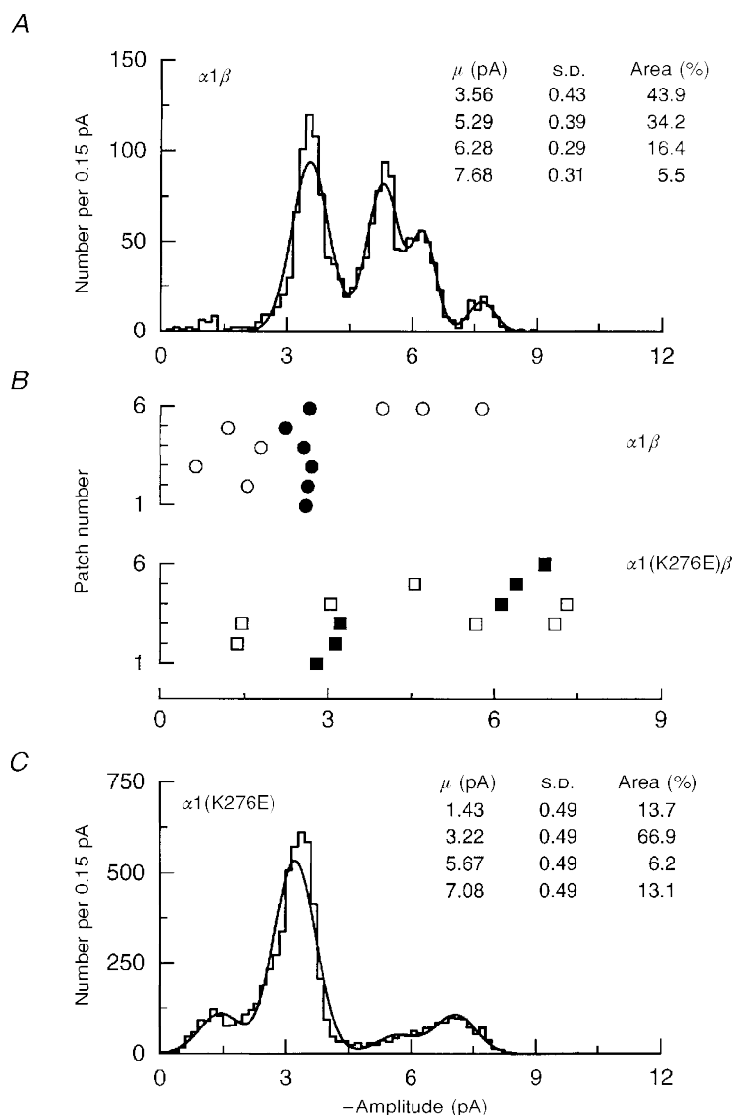


Figure 5. Amplitudes of wild-type and mutant single-channel currents

The histograms in *A* and *C* show the distribution of amplitudes of channel openings longer than three times the rise time of the filter in a wild-type $\alpha 1\beta$ patch (*A*) and in a $\alpha 1(K276E)\beta$ patch (*C*). The curves superimposed on the histograms are the result of the fit of four Gaussian components to these distributions (inset: fitted parameters for each component). The raster graph in *B* shows the amplitude of the components fitted in wild-type and mutant patches (filled symbols represent the most common current amplitude level). Most patches have a main component between 3 and 4 pA, plus a higher component around 6 pA; the $\alpha 1(K276E)$ mutation does not shift conductance to lower levels.

$\alpha 1(K276E)\beta$ open periods. The overall mean open period for $\alpha 1\beta$ was 6.85 ± 1.43 ms, and for $\alpha 1(K276E)\beta$ it was 0.82 ± 0.09 ms, so open periods were about 8-fold shorter for the mutant receptor, $\alpha 1(K276E)\beta$, than for the wild-type receptor.

Analysis of bursts

In five wild-type patches there was a sufficiently large separation of individual activations of the channel for them to be analysed as bursts of closely spaced openings. The number of bursts collected was not sufficiently large in this study to enable more than two components to be fitted to the distribution of burst lengths. When bursts were defined by a critical shut time (0.2–0.5 ms), such that only the shortest shut time component was counted as ‘within burst’, the overall mean burst length was 15.5 ± 3.0 ms (range 9–24 ms, five patches). The distribution of the number of openings per burst was fitted with a mixture of two geometric distributions (one of which always had a mean near one, i.e. it represented isolated openings). The observed

overall mean number of openings per burst was 2.21 ± 0.22 ($n = 5$). A rough correction for missed shittings was applied to this (eqn (125), p. 457, in Colquhoun & Hawkes, 1995) to obtain the corrected mean open period of 4.6 ± 0.7 ms (which was taken as an estimate of $1/\alpha$), and the corrected mean number of openings per burst, which was 3.3 ± 0.4 . The latter was used to obtain a rough estimate of β (as in Colquhoun & Sakmann, 1985). The resulting estimates of the equilibrium constant for the opening reaction, E (where $E = \text{opening rate/shutting rate}; \beta/\alpha$), ranged from 10 to 53. Thus it seems that glycine, like acetylcholine, is a ‘high efficacy’ agonist. The implications of this are considered further in the Discussion.

Bursts in the $\alpha 1(K276E)\beta$ mutant were found to be less clearly defined than in the wild-type receptors at the agonist concentrations used. A short component was predominant in the distribution of burst durations (1.01 ± 0.08 ms, $n = 4$, $t_{\text{crit}} = 0.5$ ms).

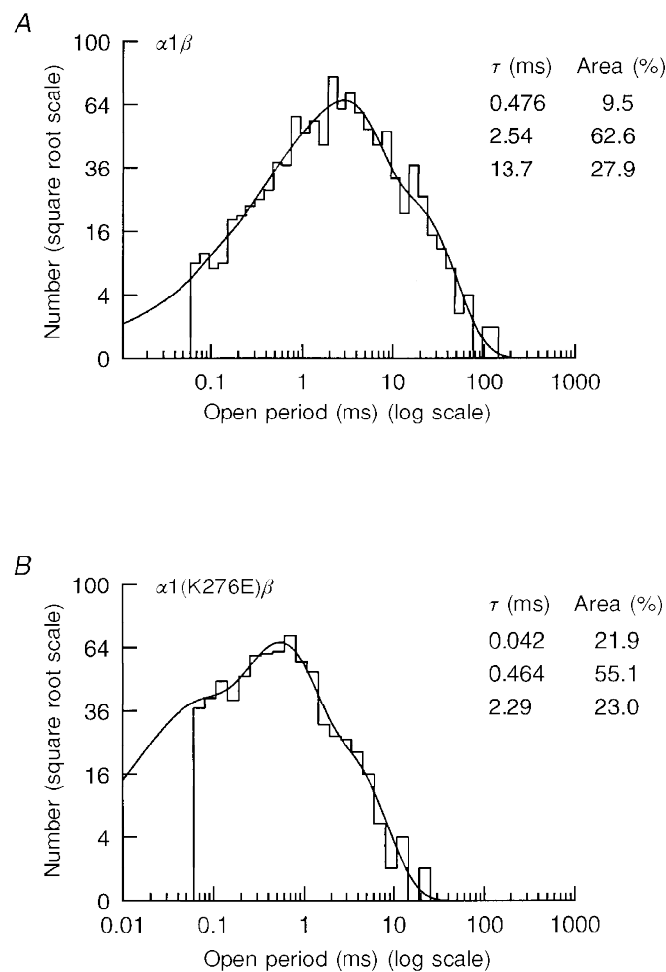


Figure 6. Apparent open periods for $\alpha 1(K276E)\beta$ and $\alpha 1\beta$ glycine receptors

The histograms display the distribution of the log duration of apparent open periods (frequency plotted on a square root scale) for an $\alpha 1\beta$ (A) and an $\alpha 1(K276E)\beta$ (B) outside-out patch. The latter are shorter than the former. The continuous lines show the result of fitting each distribution with a mixture of three exponential components (estimated parameters in the inset). τ , time constant. Agonist (glycine) concentration was $3 \mu\text{M}$ ($\alpha 1\beta$) and $100 \mu\text{M}$ ($\alpha 1(K276E)\beta$).

Table 2. Analysis of open periods

Receptor	τ_1 (ms)	Area ₁ (%)	τ_2 (ms)	Area ₂ (%)	τ_3 (ms)	Area ₃ (%)	Overall mean (ms)
$\alpha 1\beta$	0.332 ± 0.099 (5)	15.0 ± 5.2	2.41 ± 0.54 (5)	55.4 ± 5.8	13.4 ± 1.7 (5)	29.6 ± 9.3	6.87 ± 1.43 (5)
$\alpha 1(K276E)\beta$	0.072 ± 0.020 (3)	24.0 ± 3.2	0.485 ± 0.090 (6)	65.5 ± 4.3	2.50 ± 0.43 (6)	22.50 ± 4.5	0.82 ± 0.09 (6)

The time constant (τ) and area values were obtained from fitting the open period distributions with a mixture of three exponential densities, and each is expressed as mean \pm s.d. of mean, with the number of patches shown in parentheses. The last column is the mean of the τ values weighted by the relative area obtained from each fit. Agonist (glycine) concentrations were 3–10 μ M and 100 μ M for $\alpha 1\beta$ and $\alpha 1(K276E)\beta$, respectively. The total number of open periods fitted was 3814 for the wild-type and 12403 for the mutant.

DISCUSSION

Physiological effects of the $\alpha 1(K276E)$ mutation

The glycine receptor is a member of the nicotinic ligand-gated ion channel superfamily, and mediates inhibitory inputs to neurones primarily in the spinal cord and brain stem, although glycine receptor subunits have been identified by *in situ* hybridization in other regions of the central nervous system (Malosio, Marquèze-Pouey, Kuhse & Betz, 1991; Watanabe & Akagi, 1995). In its native form, the adult glycine receptor is thought to be a heteromeric pentamer composed of an α and a β subunit (Langosch *et al.* 1988) with a proposed stoichiometry of 3:2 (Kuhse *et al.* 1993). We have co-expressed the $\alpha 1$ and β subunits of human glycine receptor to mimic the native adult receptor.

Most forms of hyperekplexia described in the literature, including the one with the K276E mutation, are inherited in an autosomal dominant manner, so affected individuals will be heterozygous at the GLRA1 locus. Thus, they are likely to have glycine receptors containing a mixture of wild-type and mutant $\alpha 1$ subunits. There is no reason to suspect that the mutant or wild-type subunits will have any preferential assembly, so the postsynaptic membrane will probably have some receptors that contain all wild-type subunits, some with all mutant subunits and some with a mixture of wild-type and mutant subunits. The functional response is therefore likely to lie somewhere between the wild-type and the all mutant.

Because the decay time course of glycine-mediated synaptic currents is probably determined mainly by the mean burst length of synaptic receptors, it is to be expected that the presence of a mixed mutant–wild-type receptor population will result in a change in the decay time constants of the IPSC (for a more precise version of this statement, see eqn (2.48) in Colquhoun, Hawkes, Merlushkin & Edmonds, 1997). For spinal neurones of adult (P22) rats in which IPSCs are probably mediated by heteromeric $\alpha 1\beta$ receptors, the decay time constant was found to be 10.2 ms (Takahashi, Momiyama, Hirai, Hishinuma & Akagi, 1992). In the present

study, with human $\alpha 1\beta$ receptors, we found a mean burst length (activation length) of 15.5 ms, which is not greatly different from the IPSC decay rate in rat. For the mutant $\alpha 1(K276E)\beta$ receptors the overall mean burst length was much shorter (1.01 ± 0.08 ms, $n = 4$, $t_{crit} = 0.5$ ms) This is a little longer than the overall mean open period of 0.82 ms (Table 2). The shorter burst length suggests that mutant channels would produce a much briefer (more rapidly decaying) IPSC than wild-type. This, to the extent that it is shorter than the membrane time constant, will result in a smaller IPSP and so a decreased inhibitory glycinergic input. The interpretations discussed below might lead one to expect a slower component in the burst length distribution for mutant receptors, but if this exists it is too small to be detected, and would have little influence on the IPSC time course.

How severe the consequences of such an impairment in glycine receptor function are *in vivo* will depend on whether other inhibitory mechanisms (in particular GABAergic) can compensate for a defective glycine-mediated synaptic transmission. In the spinal cord, glycine can be co-localized with GABA in axonal presynaptic terminals (Maxwell, Todd & Kerr, 1995) which are opposed by postsynaptic membranes that often contain both glycine and GABA_A receptors (Triller, Cluzaud & Korn, 1987; Todd, Watt, Spike & Sieghart, 1996). This may be why a homozygous null mutation in the $\alpha 1$ subunit of the glycine receptor is not lethal in man (Brune *et al.* 1996), and why the benzodiazepine clonazepam (which enhances GABAergic inhibition) can improve neonatal hypertonia and attenuate the startle response in hyperekplexia patients (Ryan *et al.* 1992).

Why is the function of the mutant receptor impaired?

Inferences from equilibrium concentration–response curves. Usually, as we find below, it is not possible to be sure how the receptor is affected by the mutation from whole-cell equilibrium concentration–response curves alone. Nevertheless, useful hints can be obtained. In our case the mutant channels show a considerable increase in EC_{50} and

decrease in Hill coefficient, compared with the wild-type. This alone is sufficient to suggest that the conformation change which results in the opening and shutting (the 'gating') of the mutant channel is impaired by the mutation, in the sense that the equilibrium for this reaction is shifted towards the shut conformation. The observation that the equilibrium constant for strychnine binding is essentially unaffected by the mutation suggests, in so far as glycine and strychnine bind at or near the same site, that there is no drastic effect on the structure of the agonist-binding site.

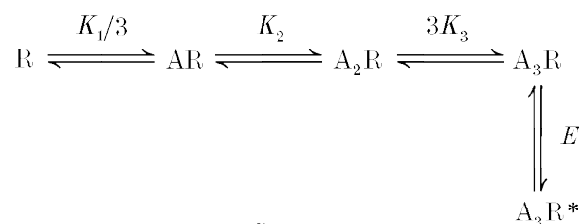
Changes in the observed maximum response. The finding that the mutant receptor appears to have a much reduced maximum response (Table 1) also suggests that the mutation impairs gating. Observation of a change in maximum response is a particularly valuable aid to interpretation of the effects of a mutation, but unfortunately it is also particularly difficult to be sure of such observations in mutant studies. For a start, the responses are invariably affected to some extent by desensitization, so the maxima fitted to curves (as in Figs 2 or 7) are unlikely to be entirely reliable (especially if the mutation affects desensitization rates). A still more serious problem is the lack of any certain knowledge of the number of functional surface receptors. The cRNA concentrations are measured only approximately, and the efficiency of their translation, assembly and insertion into functional receptors is unknown: these may be different for different batches of cRNA preparations and for different batches of oocytes. Unfortunately it is not possible to measure surface expression by strychnine binding in oocytes, but binding studies with the $\alpha 1(K276E)$ mutant expressed as a homomer in HEK 293 cells (Lynch *et al.* 1997) suggest that in this system the expression is not impaired by the mutation. A third problem, in general, in the interpretation of changes in the maximum whole-cell response concerns the possible effects of mutations on the single-channel conductance, any change in which would invalidate fitting of the results if it were not known and appropriate correction made. In the present case, however, the average single-channel conductance is similar for wild-type and mutant channels.

The possible distortion of the curves by desensitization has been noted above. The observation of faster desensitization for the wild-type might result in a shift to the left and reduction of EC_{50} , so the true increase in EC_{50} might be somewhat smaller than observed, and the true reduction in maximum response might be larger than observed. The former would not have much effect on our qualitative conclusions about mechanism, and the latter would reinforce them.

Fitting a sequential mechanism at equilibrium. It was shown in Fig. 2 that our results can be fitted adequately over the observed range by the Hill equation (for which the Hill plot $\log(y/(y_{\max} - y))$ against $\log[A]$, is a straight line). The Hill equation is, however, entirely empirical and does not represent any physically realistic mechanism. For any

real mechanism the Hill plot will not be a straight line, so its slope (the Hill slope) will be a function of agonist concentration. If we now ask whether the glycine-binding site is affected by the mutation, in addition to an effect on channel gating, it becomes essential to make some postulates concerning how the channel actually works. There is no other way to come to firm conclusions. The problem is that no detailed kinetic mechanism has yet been verified for the glycine receptor, although Twyman & Macdonald (1991) have made a helpful start on doing so. Faced with this dilemma, we have chosen to try several plausible mechanisms and to see what conclusions, if any, can be drawn that are independent of the details of the mechanism. We shall now show that the qualitative conclusion, that the effect of mutation is largely a result of impaired gating, is indeed independent of such details.

It seems likely that the heteromeric receptor has three α subunits and two β subunits (Kuhse *et al.* 1993), so we shall investigate two plausible mechanisms that involve binding of three agonist molecules. The simplest mechanism would consist of the binding of three glycine molecules (A) to the receptor (R) followed by a conformation change to the open state. This may be represented as follows.



Scheme 1

The microscopic equilibrium constants for the first, second and third binding reactions are denoted K_1 , K_2 and K_3 (the macroscopic constants are shown in Schemes 1 and 2), and the equilibrium constant for the opening reaction is denoted E (defined as opening rate/shutting rate = β/α). This mechanism is certainly too simple, if only because it has only one open state, whereas three components are needed to fit open period distributions (see Results, and Twyman & Macdonald, 1991), but even this leads to the same qualitative conclusion as more complex mechanisms discussed below.

What controls the Hill slope in the sequential mechanism? It is sometimes asked what can be concluded from the observed decrease in the Hill slope of the dose-response curves. A surprisingly simple answer to this question can be given for one class of mechanisms (and is demonstrated in the Appendix). For mechanisms that involve binding of two or more agonist molecules followed by channel opening, the Hill slope at the EC_{50} is influenced by two things: (a) the efficiency of channel gating as measured by the equilibrium constant(s) (denoted E below) for the isomerization between shut and open conformations, and (b) the extent of co-operativity in the binding reaction

itself, as measured by the inequality of the microscopic equilibrium constants for the binding steps. If the latter effect is absent (i.e. we assume that all the binding constants are the same, $K_1 = K_2 = K_3 = K$ say, and co-operativity arises entirely from there being a concerted conformation change), then it is easy to show (see Appendix) that (a) the EC_{50} depends on both K and E , (b) the Hill slope, expressed as a function of agonist concentration, depends only on K (and concentration), not on E , but (c) the Hill slope measured at the EC_{50} depends only on E , not on K . Thus a reduction in the Hill slope at the EC_{50} , as observed here, could not (within our assumptions) be produced by a change in binding alone, and strongly suggests an impairment of channel gating (we cannot, of course, infer from this observation alone that agonist binding does not change as well as there being an impairment in gating).

The foregoing result, though simple and elegant, assumes that the binding constants are all equal. This assumption is also made in the Monod–Wyman–Changeux (MWC; Monod, Wyman & Changeux, 1965) mechanism (see below), but we prefer not to make this assumption initially, because there is no reason to think it is true. Indeed, for the best-understood receptor, the muscle-type nicotinic receptor, it is probably not true (see Edmonds, Gibb & Colquhoun, 1995, for review). However, in order to reduce the number of arbitrary parameters in Scheme 1 to a realistic level, we have simplified the problem slightly by supposing that there is a constant ratio R between successive binding constants, such that

$$R = \frac{K_1}{K_2} = \frac{K_2}{K_3} \tag{3}$$

Thus, the simple assumption of equal binding constants corresponds to $R = 1$, whereas $R > 1$ implies positive co-operativity in the binding reaction, taken in isolation. This scheme (eqn (A1) in Appendix) was used to fit the concentration–response curves for the heteromeric receptor that were shown in Fig. 2. Before fitting, each curve was multiplied by the mean maximum response (given in Table 1) to remove the normalization. The curves so obtained are shown in Fig. 7.

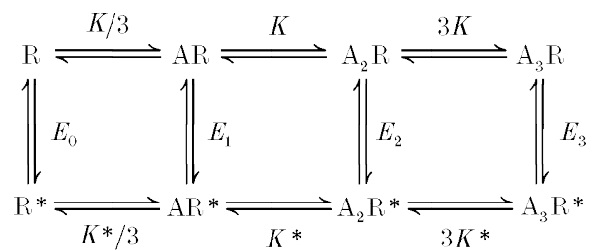
The values of K_1 , R and E were estimated separately for wild-type and mutant, but the seventh parameter, the maximum possible response (that which corresponds to $P_{\text{open}} = 1$) was assumed to be the same for wild-type and mutant, i.e. the number of channels, and their conductance, were assumed to be the same for both (although, as discussed above, this is at best an approximation).

The results of the fit (Fig. 7, legend) indicate that the effect of the mutation is largely to decrease E , i.e. to impair gating. However the data are not sufficient to determine precisely all of the parameters for the wild-type receptor (this is obvious from the large standard deviations and the very strong correlations between the parameter estimates, and from the fact that the estimates are sensitive to the

initial guesses). If the fit is repeated with the value of E for the wild-type receptor fixed at any value above ten or so, the results are visually indistinguishable from the free fits (above), but the other parameters are then reasonably well determined, and whatever value E is fixed at, the same general conclusion, that binding is little affected by the mutation, is reached. This uncertainty in the value of E for the wild-type receptor results largely from the fact that any value of E above ten or twenty predicts a similar maximum response (see eqn (A3) in Appendix). Independent evidence concerning the value of E for the wild-type would clearly be a great help in interpreting the results, and this can be found from single-channel results as described below.

Fitting the MWC mechanism

In view of the evidence for there being three open states (e.g. Twyman & Macdonald, 1991), it is important to see whether this might affect the conclusions. The simplest (fewest free parameters) mechanism of this sort is that proposed by Monod *et al.* (1965). This can be written as follows.



Scheme 2

In this case K is the equilibrium constant for binding to the shut state (R), and K^* is the equilibrium constant for binding to the open state (R^*). The equilibrium constants for gating are denoted by E_i for the receptor with i agonist molecules bound. Thus, E_0 refers to spontaneous openings of unliganded receptors (it is denoted $1/L$ in the MWC literature, but the reciprocal definition is more consistent with most of the literature on receptor mechanisms). The fact that E_0 refers to an inherent property of the receptor, independent of the nature of the agonist, makes this approach aesthetically satisfying, but unfortunately truth matters more than aesthetics and the assumption of equal binding constants is rather arbitrary (though the analysis above showed no evidence for strong co-operativity in binding). Fitting the MWC mechanism to the data gives a fit almost as good as that shown in Fig. 7 (maximum log likelihood, -2.84). Again the fit was not really determinate for the wild-type, for the same reasons as above, but gave for the wild-type: $K = 0.62 \pm 0.41$ mM, $R = K/K^* = 376 \pm 611$, and $E_0 = 1.2 \times 10^{-6}$; and for the mutant: $K = 1.6 \pm 0.2$ mM, $R = K/K^* = 8.8 \pm 2.0$, and $E_0 = 1.5 \times 10^{-4}$. These results imply that for the wild-type, $E_3 = E_0 (K/K^*)^3 = 65$ (large, like the value of E from the fit of

Scheme 1), and for the mutant, $E_3 = 0.105$ (very similar to the value of E from the fit of Scheme 1). This result is satisfactory to the extent that both E_0 values predict very low rates of spontaneous opening (no unambiguous spontaneous openings were seen), but note that E_0 seems to

change in the unexpected direction, being larger for the mutant. If the data are fitted on the assumption that only the selectivity (K/K^*) of binding for open and shut state changes in the mutant, the fit is substantially worse (maximum log likelihood, -4.48), and when it is fitted on the assumption

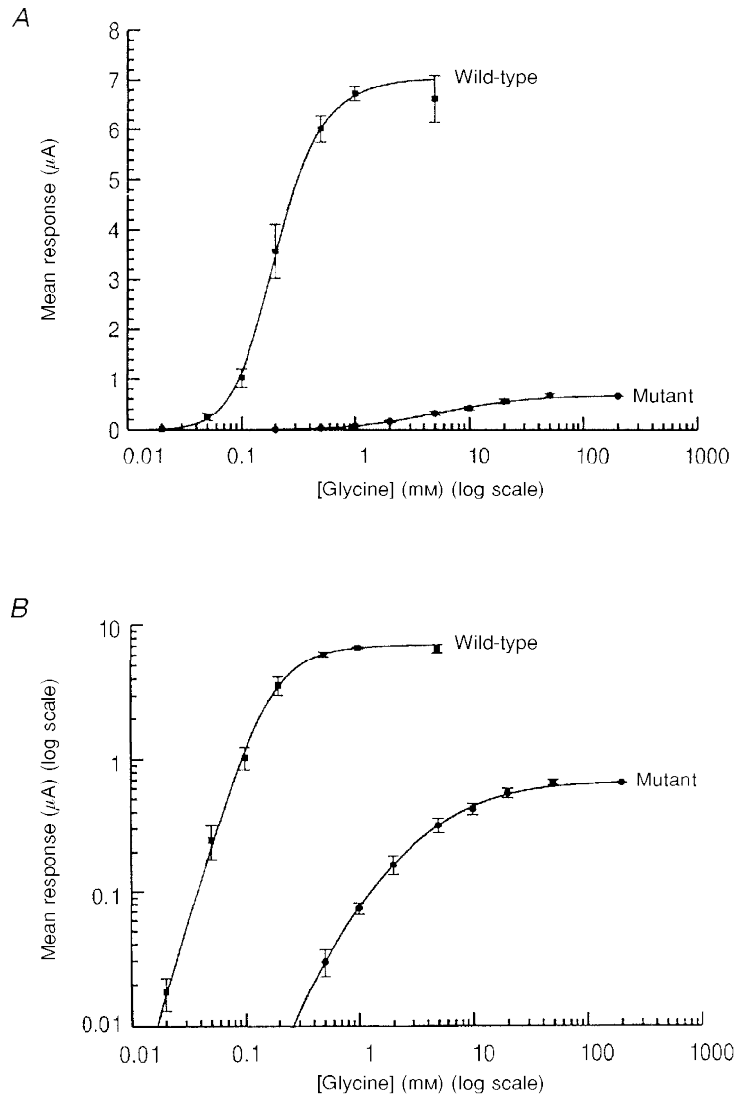


Figure 7. Fit of a mechanism to the concentration-response curves for heteromeric receptors

The data in both parts are the same as those shown in Fig. 2 for the heteromeric receptors, except that the values have been multiplied by the mean maximum currents given in Table 1. In this case the results have been fitted with the three binding site mechanism described in the Discussion (see Scheme 1). Equation (A1) was fitted, rather than the Hill equation used in Fig. 2, with the simplification that we took $R = K_1/K_2 = K_2/K_3$ (see description in the text). Thus seven parameters were simultaneously fitted to the two curves; namely separate values of K_1 , R and E for each and a common maximum, y_{\max} (which is not the maximum for either curve, but the current that would be achieved if all channels were open). *A*, response plotted against $\log(\text{concentration})$. *B*, the same data and fit as in *A*, but plotted using $\log(\text{response})$, to show more clearly the quality of the fit to the mutant receptor data. The result of the fit was $K_1 = 0.47 \pm 0.88$ mM, $R = 0.93 \pm 1.4$ and $E = 42 \pm 123$ for the wild-type channel, and $K_1 = 0.14 \pm 0.11$ mM, $R = 0.27 \pm 0.13$ and $E = 0.103 \pm 0.010$ for the mutant, with a maximum log likelihood of -2.11 . The weights for the fit were calculated from the standard deviations of the points, as indicated by the error bars on the graph, and these were the basis for the calculation of the errors (from the observed information matrix). These values imply, from eqn (3), that for wild-type, $K_2 = 0.50$ mM and $K_3 = 0.54$ mM; and for mutant, $K_2 = 0.52$ mM and $K_3 = 1.9$ mM.

that only E_0 changes in the mutant, the fit is worse still (maximum log likelihood, -7.69). The results still suggest a large change in gating for the fully liganded channel with little change in binding to the shut state, but suggest, in so far as the MWC mechanism is correct, that this results largely from a decrease, in the mutant, of the selectivity for binding to the open state, rather than from a change in E_0 .

Inferences from single-channel measurements. Single-channel recordings show that there is no decrease in the mean current carried by one channel while it is open, but the mutant channels stay open, on average, for a shorter time than the wild-type (see above). Since the mean open time, in the class of mechanisms exemplified in Scheme 1, is $1/\alpha$, this suggests that the K276E mutation causes an increase in α , and hence a decrease in E (as long as β is not increased too). This suggests, rather directly, that gating is impaired. We have measured open times at only one agonist concentration, which might be thought to be a problem in view of the demonstration by Twyman & Macdonald (1991) that open times are concentration dependent; however, they have shown clearly that the concentration dependence arises from a change in the relative areas of the three components in the distribution, but that the time constants of the three components are not concentration dependent. We find very obvious changes in the time constants, so this could not be simply a concentration effect.

It was pointed out above that if an independent estimate of the gating constant (or 'efficacy') E could be obtained, then the interpretation of the concentration–response curves would be much more secure. In the future, measurements of the absolute maximum may become possible by determining absolute P_{open} values from one-channel patches. In the meantime, the general conclusion that E is quite large for the wild-type channel is confirmed by our burst measurements. The rough estimates of E for the wild-type $\alpha 1\beta$ range from 10 to 53 ($n = 5$) (see the end of the Results section), which is the same sort of range that is suggested by the fitting done above and in the Appendix (bursts for the mutant receptor have not yet been sufficiently well characterized for this sort of analysis). This procedure for estimation of E from burst properties is intended only as a preliminary analysis; the existence of multiple open states, and of multiple conductance levels, has not been taken into account, and a more thorough analysis would have to be preceded by determination of a much better kinetic mechanism for the receptor than is available now, and of the concentration dependence, if any, of burst properties. More precise estimates will require further work.

All the analysis so far has been on the data for the heteromeric receptor. The concentration–response curves for the homomeric $\alpha 1$ receptor (wild-type or mutant) were fitted in a similar way, on the assumption that they contain four or five agonist-binding sites. Again, the results lead to the same qualitative conclusions.

In summary, the qualitative conclusion that the main effect of the mutation is on gating has been found to be independent of the details of the postulated mechanism, and therefore seems to be quite secure. More quantitative conclusions will have to await more detailed knowledge of mechanisms.

Other mutations in the M2–M3 loop

The other well-described hyperekplexia mutation, $\alpha 1$ (R271Q/L), has also been interpreted in terms of a change in receptor gating (Rajendra *et al.* 1995), which is accompanied by a decrease in the single-channel conductance. The same authors (Lynch *et al.* 1997) have also expressed the (homomeric) $\alpha 1$ (K276E) receptor in HEK 293 cells, and have suggested that this mutation also impairs gating, largely on the grounds that β -alanine and taurine are not partial agonists on the $\alpha 1$ (K276E) receptor (as on the wild-type) but behave like antagonists. In terms of mechanism, they are suggesting that E for these compounds is so much reduced that they are converted to competitive antagonists. In the context of mechanisms like that in Scheme 1, this does not necessarily mean that E would be similarly changed for glycine too, as is implicit in their argument. In the case of the MWC mechanism, however, a change in E_3 by a similar factor, regardless of the nature of the agonist, would be predicted, if the effect of the mutation was only to reduce E_0 . In fact, our attempt to fit the MWC mechanism above was not consistent with this view.

Other studies have also drawn attention to the M2–M3 loop and its function in the glycine receptor and related channels in the nicotinic superfamily. Mutations in the analogous regions in the chick nicotinic $\alpha 7$ receptor (D266N) and the rat nicotinic $\beta 4$ subunit (D268A, co-expressed with the bovine $\alpha 3$ subunit) both result in a decrease in maximum whole-cell currents and sensitivity to nicotinic agonists (Campos-Caro, Sala, Ballesta, Vicente-Agullo, Criado & Sala, 1996). Extensive investigation of the M2–M3 loop in the glycine receptor $\alpha 1$ subunit was carried out by Lynch *et al.* (1997), who mutated each residue in turn to alanine. This identified a number of key residues which, when mutated, also decreased the sensitivity to glycine and the maximum whole-cell current. In addition, a mutation in an analogous region of the GABA_C receptor $\rho 1$ subunit (R316A) resulted in an enhanced receptor function, interpreted as an increase in the open probability of the agonist-occupied receptor (Kusama, Wang, Spivak & Uhl, 1994). None of these studies gave any detailed mechanistic analysis, but in each case their authors suggest that this region contributes to the coupling of the binding of an agonist to the opening of the channel pore. If similarities can be drawn from the structural studies on *Torpedo* nAChRs (Unwin, 1995), it has been suggested by Lynch *et al.* (1997) that the M2–M3 loop may be a 'hinge' allowing the rotation of the M2 domain for the opening and closing of the channel pore in receptors belonging to the nicotinic superfamily.

APPENDIX

The three binding site mechanism

The mechanism in Scheme 1 implies that the fraction of channels open at equilibrium will be

$$P_{\text{open}} = \frac{E \frac{[A]^3}{K_1 K_2 K_3}}{1 + 3 \frac{[A]}{K_1} + 3 \frac{[A]^2}{K_1 K_2} + \frac{[A]^3}{K_1 K_2 K_3} (1 + E)} \quad (\text{A1})$$

For the fit done in the text, the P_{open} given by (A1) was multiplied by I_{max} , the current that would be obtained when $P_{\text{open}} = 1$; this was taken to be the same for wild-type and mutant, and was estimated from the data. The equations for the EC_{50} and Hill slope in this case are too long to be given explicitly here.

The fit shown in Fig. 7 showed no evidence for strong cooperativity in the binding reaction, so it is reasonable to consider next the simpler case in which all binding constants are supposed to be equal (K , say). If we define the agonist concentration, normalized with respect to its binding equilibrium constant, as

$$c_A = \frac{[A]}{K},$$

then the fraction of open channels at equilibrium will be given by

$$P_{\text{open}} = \frac{E c_A^3}{1 + 3c_A + 3c_A^2 + c_A^3 (1 + E)}, \quad (\text{A2})$$

which increases to a maximum of

$$P_{\text{max}} = \frac{E}{1 + E}, \quad (\text{A3})$$

as concentration is increased. The EC_{50} (concentration needed to achieve 50% of this maximum) is

$$EC_{50} = K_A \frac{1 + (2 + E)^{1/3} + (2 + E)^{2/3}}{1 + E}, \quad (\text{A4})$$

which depends, of course, on both binding (K_A) and on gating (E). The Hill slope is not constant, but, as a function of normalized agonist concentration, is given by

$$n_H = 3 \frac{1 + 2c_A + c_A^2}{1 + 3c_A + 3c_A^2}. \quad (\text{A5})$$

Substitution with eqn (A4) gives the Hill slope at the EC_{50} as

$$n_{H50} = \frac{8 + (6 + 3E)(2 + E)^{1/3} + (5 + 2E)(2 + E)^{2/3} + 6E + E^2}{3 \left[19 + (15 + 6E)(2 + E)^{1/3} + (12 + 3E)(2 + E)^{2/3} + 11E + E^2 \right]}. \quad (\text{A6})$$

The remarkable thing about this result is that it depends only on E (in this case, where the binding constants are supposed to be all the same, though not in general). It increases from 1.24 up to 3 as E increases.

Fitting this simpler mechanism gave a noticeably worse fit than that shown in Fig. 7 (maximum log likelihood, -7.85), as might be expected on the grounds that five rather than seven free parameters are fitted. However the fit was still tolerable and the results were $K = 0.49 \pm 0.22$ mM and $E = 39 \pm 47$ for the wild-type channels and $K = 1.17 \pm 0.066$ mM and $E = 0.102 \pm 0.008$ for the mutant. These results are qualitatively consistent with those shown in Fig. 7; almost all the effects of the mutation seem to be on gating.

ARUNLAKSHANA, O. & SCHILD, H. O. (1959). Some quantitative uses of drug antagonists. *British Journal of Pharmacology and Chemotherapy* **14**, 47–58.

BAXTER, P., CONNOLLY, S., CURTIS, A., SPENCER, V., RAVINDRA NATH, C., BURN, J. & GARDNER-MEDWIN, D. (1996). Co-dominant inheritance of hyperekplexia and spastic paraparesis. *Developmental Medicine and Child Neurology* **38**, 739–743.

BORMANN, J., RUNDSTRÖM, N., BETZ, H. & LANGOSCH, D. (1993). Residues within transmembrane segment M2 determine chloride conductance of glycine receptor homo- and hetero-oligomers. *EMBO Journal* **12**, 3729–3737.

BRUNE, W., WEBER, R. G., SAUL, B., VON KNEBEL-DOBERITZ, M., GROND-GISBACH, C., KELLERMAN, K., MEINCK, H. M. & BECKER, C. M. (1996). A GLRA1 null mutation in recessive hyperekplexia challenges the functional role of glycine receptors. *American Journal of Human Genetics* **58**, 989–997.

CAMPOS-CARO, A., SALA, S., BALLESTA, J. J., VICENTE-AGULLO, F., CRIADO, M. & SALA, F. (1996). A single residue in the M2-M3 loop is a major determinant of coupling between binding and gating in neuronal nicotinic receptors. *Proceedings of the National Academy of Sciences of the USA* **93**, 6118–6123.

COLQUHOUN, D. & FARRANT, M. (1993). The binding issue. *Nature* **366**, 510–511.

COLQUHOUN, D. & HAWKES, A. G. (1994). The interpretation of single channel recordings. In *Microelectrode Techniques. The Plymouth Workshop Handbook*, ed. OGDEN, D. C., pp. 141–188. The Company of Biologists, Cambridge, UK.

COLQUHOUN, D. & HAWKES, A. G. (1995). The principles of the stochastic interpretation of ion channel mechanisms. In *Single Channel Recording*, ed. SAKMANN, B. & NEHER, E., pp. 397–482. Plenum Press, New York.

COLQUHOUN, D., HAWKES, A. G., MERLUSHKIN, A. & EDMONDS, B. (1997). Properties of single ion channel currents elicited by a pulse of agonist concentration or voltage. *Philosophical Transactions of the Royal Society A* **355**, 1–44.

COLQUHOUN, D. & SAKMANN, B. (1985). Fast events in single-channel currents activated by acetylcholine and its analogues at the frog muscle end-plate. *Journal of Physiology* **369**, 501–557.

COLQUHOUN, D. & SIGWORTH, F. J. (1995). Fitting and statistical analysis of single-channel records. In *Single Channel Recording*, ed. SAKMANN, B. & NEHER, E., pp. 483–587. Plenum Press, New York.

EDMONDS, B., GIBB, A. J. & COLQUHOUN, D. (1995). Mechanisms of activation of muscle nicotinic acetylcholine receptors, and the time course of endplate currents. *Annual Review of Physiology* **57**, 469–493.

- ELMSLIE, F. V., HUTCHINGS, S. M., SPENCER, V., CURTIS, A., COVANIS, T., GARDINER, R. M. & REES, M. (1996). Analysis of GLRA1 in hereditary and sporadic hyperekplexia: a novel mutation in a family cosegregating for hyperekplexia and spastic paraparesis. *Journal of Medical Genetics* **33**, 435–436.
- GRENNINGLOH, G., SCHMIEDEN, V., SCHOFIELD, P. R., SEEBURG, P. H., SIDDIQUE, T., MOHANDAS, T. K., BECKER, C.-M. & BETZ, H. (1990). Alpha subunit variants of the human glycine receptor: primary structures, functional expression and chromosomal localization of the corresponding genes. *EMBO Journal* **9**, 771–776.
- HANDFORD, C. A., LYNCH, J. W., BAKER, E., WEBB, G. C., FORD, J. H., SUTHERLAND, G. R. & SCHOFIELD, P. R. (1996). The human glycine receptor β subunit: primary structure, functional characterisation and chromosomal localisation of the human and murine genes. *Molecular Brain Research* **35**, 211–219.
- KRIEG, P. A. & MELTON, D. A. (1984). Functional messenger RNAs are produced by SP6 *in vitro* transcription of cloned cDNAs. *Nucleic Acids Research* **12**, 7057–7070.
- KUHSE, J., LAUBE, B., MAGALEI, D. & BETZ, H. (1993). Assembly of the inhibitory glycine receptor: Identification of amino acid sequence motifs governing subunit stoichiometry. *Neuron* **11**, 1049–1056.
- KURCZYNSKI, T. W. (1983). Hyperekplexia. *Archives of Neurology* **40**, 246–248.
- KUSAMA, T., WANG, J.-B., SPIVAK, C. E. & UHL, G. R. (1994). Mutagenesis of the GABA $\rho 1$ receptor alters agonist affinity and channel gating. *NeuroReport* **5**, 1209–1212.
- LANGOSCH, D., LAUBE, B., RUNDSTRÖM, N., SCHMIEDEN, V., BORMANN, J. & BETZ, H. (1994). Decreased agonist affinity and chloride conductance of mutant glycine receptors associated with human hereditary hyperekplexia. *EMBO Journal* **13**, 4223–4228.
- LANGOSCH, D., THOMAS, L. & BETZ, H. (1988). Conserved quaternary structure of ligand-gated ion channels: The postsynaptic glycine receptor is a pentamer. *Proceedings of the National Academy of Sciences of the USA* **85**, 7394–7398.
- LYNCH, J. W., RAJENDRA, S., BARRY, P. H. & SCHOFIELD, P. R. (1995). Mutations affecting the glycine receptor antagonist transduction mechanism convert the competitive antagonist, picrotoxin, into an allosteric potentiator. *Journal of Biological Chemistry* **270**, 13799–13806.
- LYNCH, J. W., RAJENDRA, S., PIERCE, K. D., HANDFORD, C. A., BARRY, P. H. & SCHOFIELD, P. R. (1997). Identification of intracellular and extracellular domains mediating signal transduction in the inhibitory glycine receptor chloride channel. *EMBO Journal* **16**, 110–120.
- MALOSIO, M.-L., MARQUÈZE-POUEY, B., KUHSE, J. & BETZ, H. (1991). Widespread expression of glycine receptor subunit mRNAs in the adult and developing rat brain. *EMBO Journal* **10**, 2401–2409.
- MAXWELL, D. J., TODD, A. J. & KERR, R. (1995). Colocalization of glycine and GABA in synapses on spinomedullary neurons. *Brain Research* **690**, 127–132.
- MONOD, J., WYMAN, J. & CHANGEUX, J.-P. (1965). On the nature of allosteric transitions: A plausible model. *Journal of Molecular Biology* **12**, 88–118.
- NIGRO, M. A. & LIM, H. C. N. (1992). Hyperekplexia and sudden neonatal death. *Pediatric Neurology* **8**, 221–225.
- PRIBILLA, I., TAKAGI, T., LANGOSCH, D., BORMANN, J. & BETZ, H. (1994). The atypical M2 segment of the β subunit confers picrotoxinin resistance to inhibitory glycine receptor channels. *EMBO Journal* **11**, 4305–4311.
- RAJENDRA, S., LYNCH, J. W., PIERCE, K. D., FRENCH, C. R., BARRY, P. H. & SCHOFIELD, P. R. (1994). Startle disease mutations reduce the agonist sensitivity of the human inhibitory glycine receptor. *Journal of Biological Chemistry* **269**, 18739–18742.
- RAJENDRA, S., LYNCH, J. W., PIERCE, K. D., FRENCH, C. R., BARRY, P. H. & SCHOFIELD, P. R. (1995). Mutation of an arginine residue in the human glycine receptor transforms β -alanine and taurine from agonists into competitive antagonists. *Neuron* **14**, 169–175.
- RAJENDRA, S. & SCHOFIELD, P. R. (1995). Molecular mechanisms of inherited startle syndromes. *Trends in Neurosciences* **18**, 80–82.
- REES, M. I., ANDREW, M., JAWAD, S. & OWEN, M. J. (1994). Evidence for recessive as well as dominant forms of startle disease (hyperekplexia) caused by mutations in the $\alpha 1$ subunit of the inhibitory glycine receptor. *Human Molecular Genetics* **3**, 2175–2179.
- RUIZ-GOMEZ, A., MORATO, E., GARCIA-CALCO, M., VALDIVIESO, F. & MAYOR, F. (1990). Localization of the strychnine binding site on the 48-kilodalton subunit of the glycine receptor. *Biochemistry* **29**, 7033–7040.
- RYAN, S. G., SHERMAN, S. L., TERRY, J. C., SPARKES, R. S., TORRES, M. & MACKEY, R. W. (1992). Startle disease, or hyperekplexia: response to clonazepam and assignment of the gene (STHE) to chromosome 5q by linkage analysis. *Annals of Neurology* **31**, 663–668.
- SCHILD, H. O. (1949). pAx and competitive drug antagonism. *British Journal of Pharmacology and Chemotherapy* **4**, 277–280.
- SCHORDERET, D. F., PESCIA, G., BERNASCONI, A. & REGLI, F. (1994). An additional family with startle disease and a G1192A mutation at the $\alpha 1$ subunit of the inhibitory glycine receptor gene. *Human Molecular Genetics* **3**, 1201.
- SHIANG, R., RYAN, S. G., ZHU, Y.-Z., FIELDER, T. J., ALLEN, R. J., FRYER, A., YAMASHITA, S., O'CONNELL, P. & WASMUTH, J. J. (1995). Mutational analysis of familial and sporadic hyperekplexia. *Annals of Neurology* **38**, 85–91.
- SHIANG, R., RYAN, S. G., ZHU, Y. Z., HAHN, A. F., O'CONNELL, P. & WASMUTH, J. J. (1993). Mutations in the $\alpha 1$ subunit of the inhibitory glycine receptor cause the dominant neurologic disorder, hyperekplexia. *Nature Genetics* **5**, 351–358.
- SIGWORTH, F. J. & SINE, S. M. (1987). Data transformations for improved display and fitting of single-channel dwell time histograms. *Biophysical Journal* **52**, 1047–1054.
- TAKAHASHI, T., MOMIYAMA, A., HIRAI, K., HISHINUMA, F. & AKAGI, H. (1992). Functional correlation of fetal and adult forms of glycine receptors with developmental changes in inhibitory synaptic receptor channels. *Neuron* **9**, 1155–1161.
- TODD, A. J., WATT, C., SPIKE, R. C. & SIEGHART, W. (1996). Colocalization of GABA, glycine, and their receptors at synapses in the rat spinal cord. *Journal of Neuroscience* **16**, 974–982.
- TRILLER, A., CLUZEAUD, F. & KORN, H. (1987) γ -Aminobutyric acid-containing terminals can be apposed to glycine receptors at central synapses. *Journal of Cell Biology* **104**, 947–956.
- TWYMAN, R. E. & MACDONALD, R. L. (1991). Kinetic properties of the glycine receptor main- and sub-conductance states of mouse spinal cord neurones in culture. *Journal of Physiology* **435**, 303–331.
- UNWIN, N. (1995). Acetylcholine receptor channel imaged in the open state. *Nature* **373**, 37–43.
- VANDEBERG, R. J., FRENCH, C. R., BARRY, P. H., SHINE, J. & SCHOFIELD, P. R. (1992). Antagonism of ligand-gated ion channel receptor: Two domains of the glycine receptor α subunit form the strychnine-binding site. *Proceedings of the National Academy of Sciences of the USA* **89**, 1765–1769.

- VIGEVANO, F., DI CAPUA, M. & DALLA BERNARDINA, B. (1989). Startle disease: an avoidable cause of sudden infant death. *Lancet* **i**, 216.
- WATANABE, E. & AKAGI, H. (1995). Distribution patterns of mRNAs encoding glycine receptor channels in the developing rat spinal cord. *Neuroscience Research* **23**, 377–382.

Acknowledgements

This work was supported by grants from The Wellcome Trust and the Medical Research Council. The authors wish to thank Dr Peter Baxter for referring the family with the K276E mutation, Heinrich Betz for the gift of the human glycine receptor $\alpha 1$ subunit and Peter Schofield for the gift of the human glycine receptor β subunit. Thanks also to Dr Frances Elmslie for clinical advice on the patient phenotype, and to Mohammed Nassar and Matthias Kneussel for their help with producing the cDNA constructs. The technical assistance of David Osborne and Barry Coppenhall of the Department of Pharmacology Instrument Workshop is gratefully acknowledged.

Corresponding author

D. Colquhoun: Department of Pharmacology, University College London, Gower Street, London WC1E 6BT, UK.

Email: D.Colquhoun@ucl.ac.uk